Integrative Biology

RSC Publishing

PAPER

View Article Online
View Journal

Cite this: DOI: 10.1039/c3ib40040a

On being the right size: scaling effects in designing a human-on-a-chip

Christopher Moraes,†[a] Joseph M. Labuz,†[a] Brendan M. Leung,†[a] Mayumi Inoue,[b] Tae-Hwa Chun[b] and Shuichi Takayama*[acd]

Received 24th February 2013,
Accepted 4th July 2013

DOI: 10.1039/c3ib40040a

www.rsc.org/ibiology

Developing a human-on-a-chip by connecting multiple model organ systems would provide an intermediate screen for therapeutic efficacy and toxic side effects of drugs prior to conducting expensive clinical trials. However, correctly designing individual organs and scaling them relative to each other to make a functional microscale human analog is challenging, and a generalized approach has yet to be identified. In this work, we demonstrate the importance of rational design of both the individual organ and its relationship with other organs, using a simple two-compartment system simulating insulin-dependent glucose uptake in adipose tissues. We demonstrate that inter-organ scaling laws depend on both the number of cells and the spatial arrangement of those cells within the microfabricated construct. We then propose a simple and novel inter-organ 'metabolically supported functional scaling' approach predicated on maintaining *in vivo* cellular basal metabolic rates by limiting resources available to cells on the chip. This approach leverages findings from allometric scaling models in mammals that limited resources *in vivo* prompt cells to behave differently than in resource-rich *in vitro* cultures. Although applying scaling laws directly to tissues can result in systems that would be quite challenging to implement, engineering workarounds may be used to circumvent these scaling issues. Specific workarounds discussed include the limited oxygen carrying capacity of cell culture media when used as a blood substitute and the ability to engineer non-physiological structures to augment organ function, to create the transport-accessible, yet resource-limited environment necessary for cells to mimic *in vivo* functionality. Furthermore, designing the structure of individual tissues in each organ compartment may be a useful strategy to bypass scaling concerns at the inter-organ level.

Insight, innovation, integration

Design of a human-on-a-chip for drug efficacy and toxicity screening must follow rational guidelines in scaling various components appropriately. Scaling on a chip presents unique challenges and opportunities, distinct from typical allometric scaling considerations. This work experimentally illustrates the connection between microtissue structure and functional scaling relationships between organ compartments, demonstrating potential relationships between intra- and inter-organ design specifications. An innovative scaling strategy is then proposed to design a human-on-a-chip for metabolic studies, and we explore the parameter space for such a system, suggesting microengineering approaches and technologies to circumvent or alleviate the practical challenges presented by constructing an appropriately scaled chip. Though designed for metabolic studies, this approach may be broadly applicable in the design of physiologically relevant humans-on-a-chip.

1. Introduction

Recent advances in microfabrication technology have enabled the production of 'organs-on-a-chip', microfabricated devices that mimic essential aspects of organ function.[1–3] Technologies that incorporate critical mechanical,[4–6] topographical[7] and material[8] cues into cell culture models can replicate *in vivo* functionality,[9,10] suggesting a promising approach for *in vitro* drug testing. Authentic recreation of these environments in an *in vitro* system presents significant ongoing challenges, but

[a] Department of Biomedical Engineering, College of Engineering, University of Michigan, 2200 Bonisteel Blvd, Ann Arbor, MI 48109, USA
[b] Department of Internal Medicine, University of Michigan Health System, 1500 E. Medical Center Drive, Ann Arbor, MI 48109, USA
[c] Macromolecular Science and Engineering Center, College of Engineering, University of Michigan, 2300 Hayward St., Ann Arbor, MI 48109, USA
[d] Division of Nano-Bio and Chemical Engineering WCU Project, UNIST, Ulsan, Republic of Korea. E-mail: takayama@umich.edu
† Equal contributions.

may enable higher quality screens for drug discovery.[3,11] Recently, the concept of combining such technologies to create an artificial ''human-on-a-chip'' has been met with great interest, as such tools will help screen potential therapies for efficacy and eliminate therapies that have toxic side-effects[12] prior to expensive clinical trials. Promising drugs identified in animal models are notoriously difficult to translate to humans due to small but significant differences in cell physiology,[13] genomic responses[14] and other factors such as lipid profiles.[15] Furthermore, the complexity of animal model systems can hinder identification of the mechanism by which the drug failed. Hence, creating an artificial, precisely-defined microscale representation of a human being will address some of these issues, and should enable higher quality screens to rapidly discover issues with efficacy or side effects of potential pharmaceuticals.

The tools to integrate multiple cell types towards a human-on-a-chip already exist, and researchers have been developing these physiologically relevant models for several years. Initially, cell culture systems involving simultaneous culture of multiple cell types in microwells connected by a static layer of fluid enabled analysis of toxicity to cells from five interacting organs.[16,17] Pioneering work by Shuler and coworkers first demonstrated the possibilities of integrating multiple microscale cultures with microfluidic systems, thereby controlling transport rates and quantities between organ compartments.[18] Similarly, others have utilized multiple connected compartments on a microfluidic chip,[19–21] or in modular bioreactors that can be connected in any desired fashion.[22,23] These approaches each use technologies that are now reasonably mature and compatible with techniques to include organ-specific microenvironmental cues into the system. Hence, significant technical progress is being made towards the possibility of recreating human organs in a microfabricated format. While such tools will initially be used to test specific hypotheses regarding toxicity mechanisms, eventually these tools may also be used to drive high-throughput discovery-based research.

Although the technology exists with which to build such devices, several issues remain with regard to implementing such human-on-a-chip models. For example, the ability of an engineered tissue construct to authentically replicate physiologically realistic function continues to be a pressing concern. In this work, we focus on a broader question regarding the design of relative organ sizes and fluidic connections within the human-on-a-chip. If the human is being scaled down to micro-proportions, should the lungs and liver scale at the same rate? In his short essay, ''On being the right size'', J. B. S. Haldane discusses the physiological complexities that must arise as a consequence of animal size.[24] Do we now adjust for these complexities when developing microscale analogs of humans? Disproportionately scaled organs on a chip will have significant negative effects on replicating human responses, particularly when those functions are dependent on interacting organ systems. For example, tegafur is a chemotherapeutic agent that becomes effective only after conversion to 5-fluorouracil by the liver.[25] If the scaled liver-on-a-chip was not of sufficient size

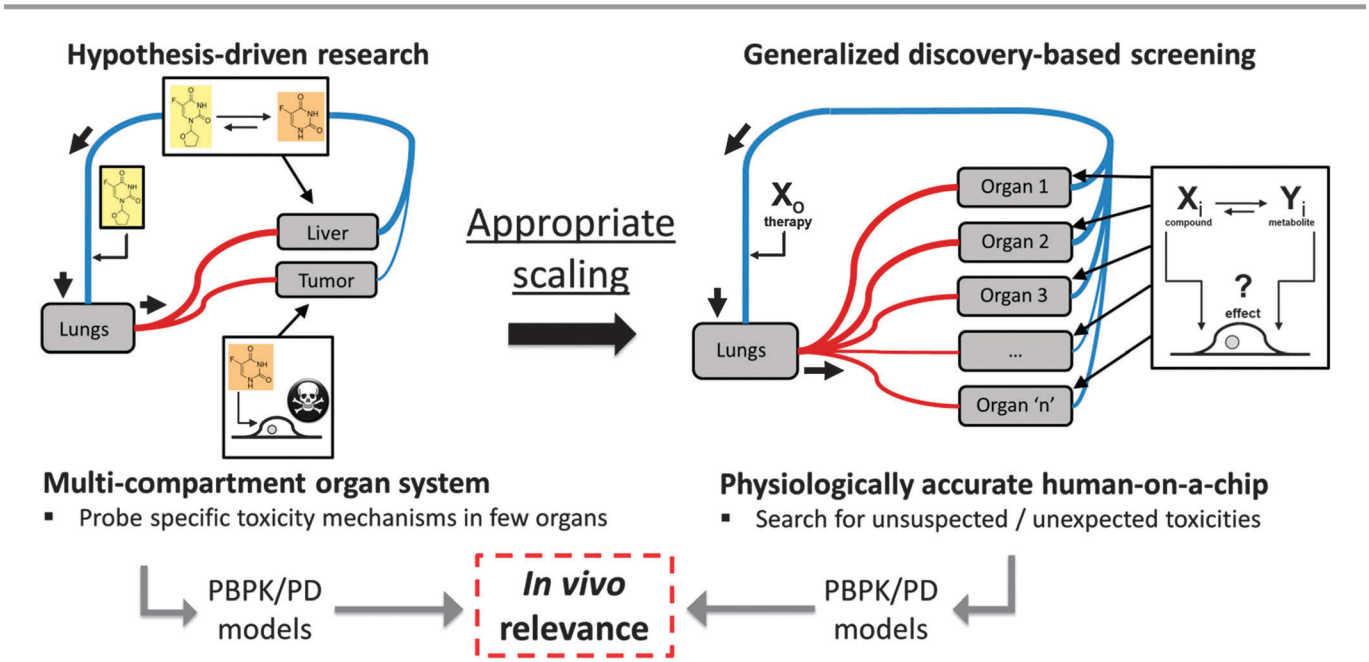

Fig. 1 Microtechnologies to generate multi-compartment organ systems have been demonstrated to effectively conduct hypothesis-driven research into suspected mechanisms of toxicity arising from actions by a few key interacting organs. By extending these approaches to include many organ systems, a ''human-on-a-chip'' may be developed. Such a system could be used to conduct generalized drug discovery screening, to identify potential toxicities prior to human clinical trials. In both cases, physiologically based pharmacokinetic and pharmacodynamic (PBPK/PD) models may be applied to determine *in vivo* relevance, but directly observing toxicities that may occur through unknown and unsuspected mechanisms between yet to be determined inter-organ interactions will require that many organ compartments be scaled appropriately, to accurately mimic physiological interactions. There is currently a lack of understanding of how to perform this ''appropriate scaling''. This article reviews scaling approaches that have been used or discussed to date and to introduce some new ideas for appropriate scaling.

to metabolize tegafur to 5-fluorouracil in quantities sufficient to kill the scaled tumor-on-a-chip, no effect would be noted. Hence, if either the tumor was disproportionately large or the liver was disproportionately small, the screen would return a false negative. Likewise, if an adipose tissue-on-a-chip was not designed to scale correctly with blood volume and with the size of the insulin-producing pancreas, humans-on-a-chip would be in a constant state of hyper- or hypoglycemia. Screening drugs in these systems would be akin to testing drugs in patients who are either diabetic or prone to severe seizures, and hence may provide results that do not translate to the broader population. Hence, this issue of 'scaling', of reducing the relative size of each organ compartment to maintain appropriate functionality of the whole system, is central to the successful design of a generalizable human-on-a-chip (Fig. 1).

In this work, we critically review existing approaches to scaling in designing microscale organ systems and conduct a simple experiment to investigate how tissue structure might influence scaling in a simple multi-compartment organ system. We then propose and develop a novel scaling methodology based on maintaining *in vivo* cellular basal metabolic rates, and expand upon a recent suggestion by Wikswo and colleagues[26] to use a 'functional scaling' approach to specify parameters in such systems. Challenges in practically implementing these models then lead us to highlight some engineering approaches that may be used to bypass the issues raised in appropriately miniaturized human physiological systems.

2. Critical review: current rational approaches to scaling multicompartment organs

While most prototype multi-organ systems to date generally do not consider the effects of scaling multiple compartments in their design,[2] two approaches have been considered in the literature: utilizing allometric scaling principles; or scaling based on organ mass and residence times to design fluid circuits between organ compartments.

Allometric scaling

Allometry is the study of the relationship between body size and shape, anatomy and physiology.[27,28] Quarter-power exponential scaling relationships between animal size and physiological parameters have been empirically determined[29–31] and mathematically supported.[32–34] These relationships, first empirically identified by Kleiber for basal metabolic rate (BMR),[30] hold reasonably true over species spanning 27 orders of magnitude in size (Fig. 2A).[35] Exponential power relationships typically follow the form

$$Y = Y_o M^{\alpha} \quad (1)$$

where Y is the physiological property, M is the mass of the organism, α is the scaling exponent, and Y_o is a constant. Although some debate has arisen as to the precise value of these scaling exponents, metabolic rate is generally considered

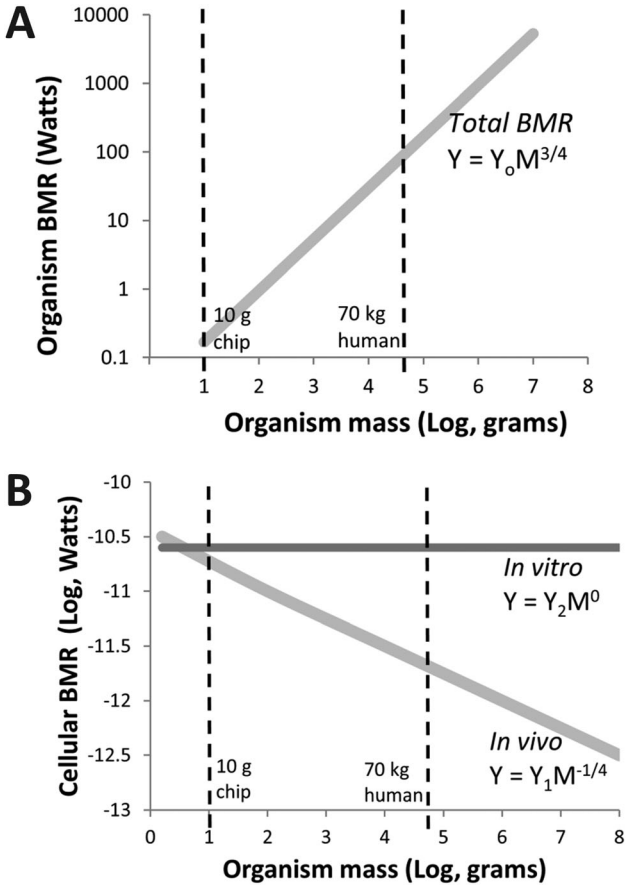

Fig. 2 Allometric scaling of basal metabolic rate with organism size. (A) Kleiber's law demonstrates that when plotted on a log–log scale, a 3/4 power scaling dependence can be observed for basal metabolic rate of animals across a wide range of sizes (graphs based on data in Kleiber[30]). (B) Distinct differences in metabolic rate per cell are found between cells within organisms of different size and those cultured *in vitro*. While cells *in vivo* scale with a −1/4 power scaling exponent, cells cultured *in vitro* significantly raise basal metabolic rate and are no longer dependent on the organism mass from which they came. These findings demonstrate that the allometric network is responsible for controlling cell function, and that metabolic rate is not an intrinsic property of the cell (graphs based on data in West *et al.*[35]).

to follow a 3/4 power scaling law, due to the presence of space-filling branching structures for resource transport.[34,36,37]

Using these scaling parameters, researchers have designed a variety of multi-organ systems by connecting a series of modular bioreactors.[22] For example, allometric scaling laws are used to estimate the size of the 'chip organism' based on the total energy output of the liver, as calculated on a per cell basis. The other compartments are scaled to maintain allometric relationships with the liver.[38] This approach has been used to study interactions between hepatocytes and endothelial cells,[39,40] and more recently between hepatocytes, adipose tissue[41] and endothelial cells.[42] While this may be useful in designing a small number of organ compartments, scaling a human down by a factor of 1000× would result in a wide range of changes in relative organ size (Y in eqn (1)), as the allometric scaling coefficient for organ volume is different for each organ. For example, within organs that serve primarily

secretory functions and would be expected to maintain their mass with respect to each other, the relative size of the pituitary gland is reduced by a factor of 0.44 (allometric scaling coefficient $\alpha = 0.68$), while the relative size of the thyroid gland is increased by a factor of 9.1 (where $\alpha = 1.1$), as recently estimated by Wikswo and colleagues.[26] Whether this 20× difference in scaled volume (and hence secretory potential) remains relevant to human physiology is unknown, but seems quite unlikely.

Significant issues underlie this interpretation and application of allometric scaling laws to the design of humans-on-chips. In general, allometry-based scaling approaches may not be valid for all tissue types, as demonstrated by recent studies showing linear scaling relationships in cellular metabolic rate amongst neurons of different species.[43–45] More specifically to designing humans-on-a-chip however, three critical concerns exist. First, as demonstrated by West, Brown and Enquist, the mathematical basis for the elegant three-quarter power scaling law is predicated on the assumption that life is sustained by hierarchical branching transport networks that are space-filling and optimized by the process of natural selection.[34,46] Organs-on-a-chip are generally not optimized for resource distribution. Hence, the transport network is not necessarily space-filling, and the structure of the engineered organ-on-a-chip can yield distinct results depending on the diffusive limit of thick tissues and underlying transport phenomena. Thus, the 3/4 power scaling exponent likely does not apply to organs-on-a-chip as their sizes are increased or decreased.

Second, these allometric calculations to design multi-organ compartments assume that the energy production by a single cell is independent of the environment in which it is placed.[38] However, allometric scaling theory also predicts that cells will maintain either (a) a constant volume or (b) a constant basal metabolic rate, with changes in total organism mass.[47] Since most cells do not change volume in different contexts, removing the cell from an animal and culturing it *in vitro* will produce significantly increased metabolic rates (Fig. 2B),[35] in agreement with both scaling theory and experimental results. Thus, cell functions are not an intrinsic feature of the cell independent of other factors, but significantly influenced by the systemic network that supports it,[48] thereby limiting this scaling approach. Unless specific steps are taken to account for these factors (such as the use of quiescent cells or resource-limited microenvironments), cells removed from the body and cultured in a human-on-a-chip no longer maintain the metabolic profiles of their *in vivo* counterparts. Hence, empirically determined allometric scaling laws for organism mass will not apply to the design of these artificial organ systems.

Third, small animals circulate blood rapidly with increased heart rates (the average heart rate of mice is 600 beats per minute, $\alpha = -0.25$). Hence, cells in this milieu exist in a resource-rich environment, with greatly increased access to re-oxygenated blood and nutrients. Speculatively, given the established influence of oxygen availability in driving cell phenotype and responses,[49] the increase in BMR of cells in small animals as a direct consequence of their size may be one of the factors contributing to the gap observed in translating drug screening results between animal and human models. This and other scaling-related differences between organisms of different size should prompt us to carefully evaluate the philosophy underlying the use of allometric scaling to design humans-on-a-chip: are these systems being designed to mimic functionality in a human, or functionality in a mouse-sized human? Mouse-sized humans would have significantly larger cellular BMR, and may present different responses to stimuli.

Hence, the practice of utilizing allometric scaling coefficients of organ volumes that are empirically determined by observing 'real' organisms may not be the most suitable method to design a human-on-a-chip, unless we consider specific factors such as the metabolic differences in cellular BMR between *in vivo* and *in vitro* cultures. Furthermore, the fact that microfabricated tissues can be structurally different from their *in vivo* counterparts can make this situation even more complicated. Will microfabricated tissues continue to maintain scaling relationships as they are miniaturized? The extent to which scaling might influence tissues of different structures remains an open question, and one which is important to address prior to designing a 'generalized' human-on-a-chip.

Scaling by organ mass and residence times

Shuler and co-workers pioneered the approach to design chamber sizes and flow rates based on organ sizes and residence times, and to use rigorous pharmacological models[12,18,25,50–52] to extract physiologically relevant information from these models. In terms of eqn (1), this approach corresponds to $\alpha = 1$, or a linear relationship between organ and organism mass. They then utilized physiologically based pharmacokinetic (PBPK) models[18] in combination with pharmacodynamic (PD) models[51] to rationally analyze the scaled system, explain observed results, and translate their findings to *in vivo* contexts. Briefly, each organ is scaled according to organ mass or volume and the flow of blood (or blood substitute) to the chambers is designed based on *in vivo* residence times (*i.e.*, the amount of time required for the volumetric flow through a chamber to equal the volume of the chamber). Each organ is then modeled as a separate compartment, in which ordinary differential equations can be used to calculate the compartment-specific and time-dependent concentration of drugs and metabolites. When coupled with fluid transport equations, this simple but powerful approach can be used to understand drug and metabolite concentration profiles and residence times for chambers of different sizes. In this way, multiple organs can be analyzed to test specific hypotheses surrounding a particular drug, and translate the results to *in vivo* situations.

Scaling based on organ mass ratios and the subsequent application of PBPK/PD models is amongst the most rigorous approaches to date, and provides excellent insight into specific disease model systems. While this method is extremely useful to test very specific hypotheses, it is challenging to extend this scaling approach towards the initial design of a generalized and appropriately scaled human-on-a-chip for discovery-based screening. In existing works, initial chip design is typically based on scaling to maintain organ mass ratios and fluid

Table 1 Physical parameters required to maintain a consistent volume-to-area scaling factor for a 73 kg male

Organ	Organ mass (g)	Organ area (m^2)	V/A ratio ($g\ m^{-2}$)	V/A scaling factor: 10^6	
				Mass (mg)	Area (mm^2)
Lung	555	~70	7.93	0.555	70
Liver	1876	~400	4.69	1.876	400
Heart	343	~0.02	17 155	0.343	0.02
Kidney	321	~0.0516	6223.6	0.321	0.0516
Adrenal glands	14	~0.0001	140 000	0.014	0.0001

residence times in organs suspected to play a role in the toxicity mechanism under study. Other organs of the body are implicitly included in the analysis using a single compartment that may not provide physiological functionality. While this works well in simulating a few selected organ systems, achieving a truly generalizable human-on-a-chip for discovery-based drug screening will require many organs to be included and appropriately scaled, as the mechanism of toxicity will be unknown and unsuspected. Scaling based on organ size alone neglects differences arising from surface area to volume ratios, which can play a considerable role in organ function. Scaling approaches based on maintaining the ratio between surface area and volume in miniaturized organs result in organ dimensions that are practically unrealistic to achieve (selected examples are demonstrated in Table 1). In these examples, surface areas spanning several orders of magnitude are necessary, and will be challenging to practically realize in any format, particularly given the low organ volumes that accompany the requirements for large surface areas. If these limitations in the initial design of an appropriately scaled human-on-a-chip can be overcome, then the use of PBPK/PD models will be better enabled to first screen the effects of pharmaceuticals in a discovery-based experiment, and then generate specific hypotheses to study mechanism-based translation of drug action to *in vivo* environments. However, establishing the appropriate scaling parameters to effectively miniaturize a human while maintaining human-like function remains challenging.

In this work, we conduct two related studies: an experimental analysis of scaling in microengineered tissues of different structures; and a theoretical analysis of how scaling relationships might be applied to, and where necessary, circumvented to design a human-on-a-chip.

3. Experimental scaling of microengineered tissues

To investigate how tissue structure might influence scaling relationships in microfabricated circuits, we developed a simple experimental platform that can prompt multiple tissue structures to produce a functional response. We used adipose tissues of different structures and containing different cell quantities as a model system to demonstrate the relationships between scaling and organ structure.

Adipose tissues are critical regulators of systemic organism function, including the maintenance of energy balance, metabolism of hormones, and the production of adipokines and

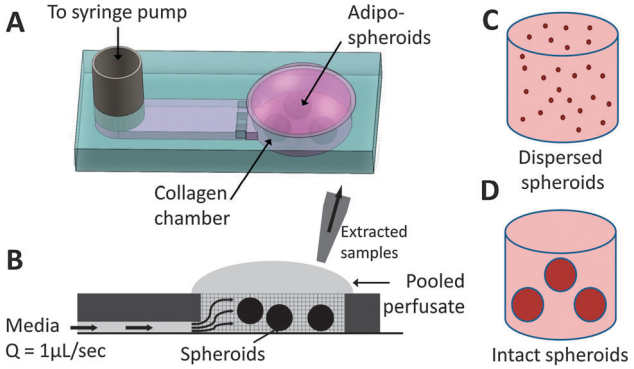

Fig. 3 Two-compartment device. (A and B) Schematics demonstrating device structure and operation. Cell- or spheroid-laden collagen is polymerized in the collagen chamber. The posts around the chamber prevent the collagen from travelling into the channels. A syringe pump forces media through the system at a volumetric flow rate Q of 1 $\mu L\ s^{-1}$, and the pooled perfusate is pipetted away at the end of the experiment. Tissue structure is manipulated by either using (C) mechanically dispersed spheroids or (D) intact spheroids encapsulated in the collagen matrix.

lipoproteins.[53] A critical purpose is to clear glucose from the bloodstream and store it as an energy source in the form of lipids. Disruption of this mechanism leads to hyperglycemia, which is the principal clinical component of diabetes mellitus. In addition, prolonged hyperglycemia causes microvascular complications, tissue inflammation, and pancreatic beta cell toxicity.[54] Hence, adipose tissue would be an important model organ to include in a human-on-a-chip.

A generally accepted *in vitro* model of adipocyte differentiation is the 3T3-L1 cell line, which undergoes adipocyte differentiation (adipogenesis) in the presence of certain hormonal cues.[55,56] Differentiation of 3T3-L1 cells is characterized by cell shape change and the accumulation of triglyceride droplets within the cytoplasm. These differentiated adipocytes are capable of insulin-dependent glucose uptake mediated by GLUT4 trafficking as found in native adipose tissues.[57] Upon differentiation and stimulation with insulin, 3T3-L1 cells display a 3- to 4-fold increase in insulin binding[58] and a 5-fold increase in glucose uptake.[59] In addition, insulin actively regulates the nutrient uptake and metabolic rate of adipocytes.[60] Hence, the adipose tissue compartment has the potential to serve as a tunable source/sink of metabolites in the design of a human-on-a-chip.

Spheroid culture systems are a convenient and robust platform that recapitulate some key aspects of physiological tissues, including 3-D cell–cell/cell–ECM interactions[61] and the presence of chemical gradients caused by diffusion limitations within the spheroid.[62] In this work, functional adipose tissues were produced by differentiating 3T3-L1 cells in hanging drop spheroid culture[63,64] and loading them into a type I collagen-filled chamber (Fig. 3A and B). Tissue structure was altered by enzymatically disrupting the spheroids to scatter the cells within the collagen-filled chamber, or by allowing the spheroids to remain intact (Fig. 3C and D). Cell number for the dispersed condition was altered by diluting the cells in ten times the volume collagen precursor upon resuspension. These simple tissues were then stimulated with insulin to study the effects of differential scaling of the system on glucose uptake.

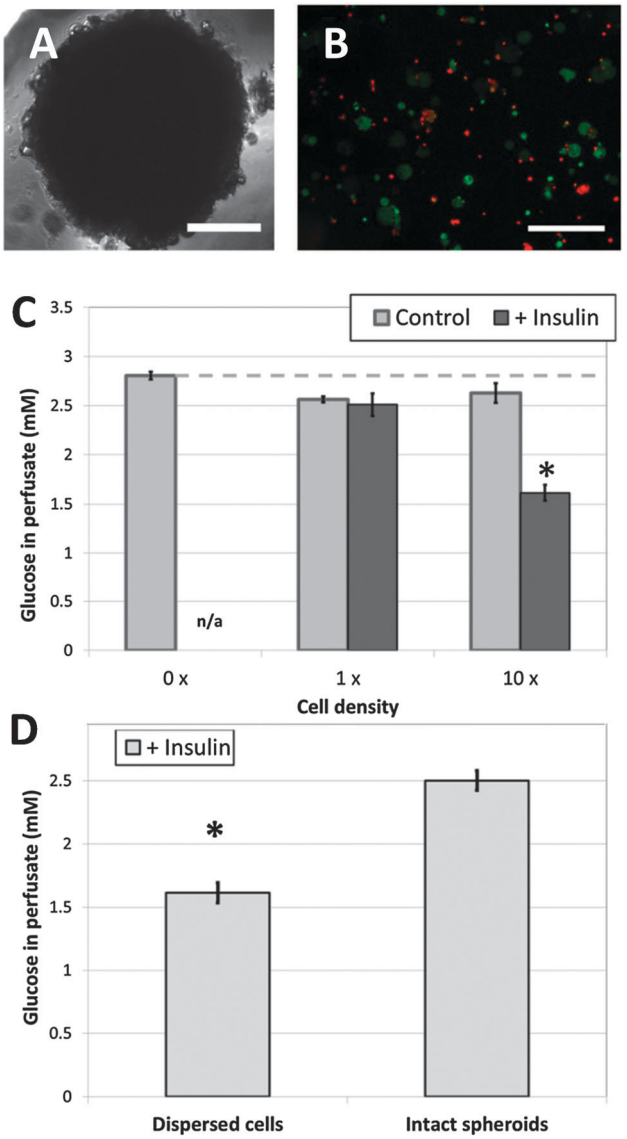

Fig. 4 Characterizing adipose function in two-compartment devices. (A) Sample bright field image of an intact adipocyte spheroid, prior to dispersion. (B) Dispersed cells assayed for viability using a LIVE/DEAD fluorescent kit (green = calcein AM stained cells, live; red = ethidium homodimer stained cells, dead; scale bar = 300 μm). (C) Dispersed spheroids were loaded into the device at varying densities (0× = no cells; 1× = cells dispersed from 0.3 spheroids; 10× = cells dispersed from 3 spheroids) and perfused with either control media or insulin-containing media. Insulin prompts significant uptake of glucose by the adipocytes in the 10× condition (*$p < 0.001$ by ANOVA as compared to all other conditions; data plotted as means ± SEM, n = 7–8). (D) Adipose tissue architecture plays a significant role in the uptake of glucose in this system. Dispersed cells from three spheroids consume significantly greater amounts of glucose (*$p < 0.001$, n = 7–8) as compared to three intact spheroids, likely due to transport limitations in intact spheroids.

The microsystem was designed to have two compartments. The blood-substitute compartment consists of insulin-supplemented HBSS, and remains constant through all experiments at ~25 μL of working volume. The tissue compartment consists of intact (Fig. 4A) or dispersed (Fig. 4B) adipogenically differentiated spheroids encapsulated in a collagen-filled chamber. To ensure that the system is scaled at the right order of magnitude to simulate a real organ, simple scaling calculations were performed. For a 1 : 1 volumetric scaling between total blood volume in a human being and the volume of blood substitute on this chip, the system represents a miniaturization factor of approximately 10^7. Hence, an isometrically scaled fat compartment should have a volume of ~100s of nL of cells.[65] We simulate this system using dispersions obtained from three adipose spheroids, the volume of which is on the order of 100 nL (labeled 10×). These dispersions were diluted by a factor of 10, to create tissues with cell volumes of ~10 nL (labeled 1×) representing an order of magnitude difference from the expected scaling approach.

A fluorescent Live/Dead viability analysis of dispersed spheroids indicates a viability of ~60%. Although it is unknown whether the reduced viability of the system arises from cell death within the core of the adipo-spheroid during maturation, or due to the dispersion process, comparisons are only made between samples drawn from the same batch of well-mixed dispersed spheroids. Dispersed spheroids are diluted to the appropriate concentration in prepolymerized collagen, loaded onto the chip, allowed to gel and stimulated with insulin. These compartments containing distinctly scaled densities of adipocytes were then stimulated with insulin to uptake glucose for 25 minutes. When sufficient insulin is present to stimulate the cells, we expected that greater numbers of cells uptake greater quantities of glucose. As demonstrated in Fig. 4C, while cells consumed a small amount of glucose from the media under perfusion conditions without insulin, no significant reduction in perfusate glucose levels was observed between the 1× (~1 million cells per mL) and 10× (~10 million cells per mL) densities of cells tested. Exposing the cells to insulin prompted a significant increase in glucose uptake for tissues with 10× cell density (*$p < 0.001$, as compared to all other conditions). This level of glucose reduction in the blood compartment is consistent with values reported in existing studies of insulin-triggered glucose uptake.[66,67]

Tissue structure may also play a significant role in altering interactions between the blood and adipocyte compartments. In order to demonstrate these interactions between organ compartments, an equivalent number of spheroids were allowed to remain intact and encapsulated within the collagen matrix. Intact spheroids do not uptake as much glucose as dispersed spheroids (Fig. 4D, $p < 0.001$), resulting in similar uptake levels as the 1× dispersed tissues ($p > 0.95$ between 10× intact spheroids and 1× dispersed cells), demonstrating that tissue architecture can significantly affect scaling relationships in microfabricated devices. Though it is possible that the dispersion procedure may reduce the viability of the cell-laden tissue, this difference would reduce the amount of glucose consumed by the tissue, thereby minimizing any experimental differences observed. Hence, because dispersion was necessary to observe differences in glucose uptake, this allows us to conclude that any differences are primarily due to transport limitations in the intact spheroids, where insulin and glucose do not have rapid diffusional access to cells in the inner core of the spheroid.

This simplified microfabricated system makes several assumptions that make it unsuitable for the design of a realistic human-on-a-chip. Fluid flow does not recirculate. Exchange of metabolites to other tissues is ignored, and no allowance is made for other interacting compartments in the system. As such, this system is not appropriate to recreate physiological functionality, but instead is designed to reveal and highlight two important points on the design of interacting organ systems. First, and not surprisingly, the number of cells present can influence physiological variables in the system. Clearly, maintaining glucose homeostasis would be crucial for any human-on-a-chip application. Here, we demonstrate that different scaling approaches between adipose tissue and blood can result in altered blood glucose levels. Second, the structure of the tissue is of critical importance in observing a scaling effect. While the system was sensitive to the number of cells, this was only true when the cells were arranged in a manner that was not transport-limited. A dispersion of adipocytes in a collagen hydrogel can be likened to vascularized fat, in which a delivery network of channels is used to overcome diffusion-limited transport of molecules. Hence, because the intact spheroids are not fitted with a space-filling vascular transportation network, they do not follow patterns predicted by even an extremely simple cell number-based scaling approach.

4. Towards a human-on-a-chip: metabolically supported functional scaling

To replicate human responses in drug discovery, we believe that cells in the human-on-a-chip must function as closely as possible to cells in the body, with an appropriately sized drug dosage.[68] At the most precise level, this approach will require careful consideration of all the parameters involved in PBPK/PD models, particularly drug adsorption, distribution, metabolism and excretion. Furthermore, precise replication of all micro-environmental design parameters, such as mechanical stimulation, gradients of oxygen, chemical and matrix proteins, and tissue structure, needs to be considered.[11] For the purpose of the following discussion, we ignore issues of microenvironmental design and focus only on aspects of scaling between multiple organ compartments in a human-on-a-chip. Here, we investigate the theoretical design of a less precise, 'generalized' representation of a human-on-a-chip, as a first-order screening system for drug toxicity, and demonstrate that scaling approaches alone cannot be easily implemented without some engineering techniques to circumvent issues of size.

The main criterion we apply to enable scaling towards a human-on-a-chip is to match the cellular BMR on the chip to cells in the body, assuming that BMR is a master regulator of cell function. This hypothesis is supported by data from allometric scaling models that show that organism size significantly influences cell BMR *in vivo*[35] (Fig. 2B), and from *in vitro* culture models that demonstrate that limiting resources forces cells to behave in a more *in vivo*-like manner.[49] If the cells present in a human-on-a-chip were to maintain *in vivo*-like metabolic phenotypes, then the human-on-a-chip should follow the empirically determined allometric trends between organs from organisms of different sizes. We further believe a focus on BMR makes particularly good sense for humans-on-a-chip for the study of metabolic disease and drugs to treat such conditions, although it may be more broadly applicable. The critical difference between this '*metabolically supported functional scaling*' approach and previous applications of allometric scaling in designing humans-on-chips is that we aim to ensure that the underlying prerequisite for allometric scaling is maintained in artificial organisms. If the human-on-a-chip organism follows the restrictions of a naturally evolved organism, then components of the human-on-a-chip should follow empirically observed allometric scaling coefficients. Hence, we propose that focusing on cellular BMR is just as critical as maintaining appropriate inter-organ size scales.

Control of BMR may be possible through a number of methods including manipulating cell proliferation potential, regulating the supply of nutrients, and controlling oxygen availability. The techniques used will be largely dictated by the specific organ under construction, the specification of which is beyond the scope of this work. We believe that control of oxygen supply may be the most broadly applicable technique, and for the purpose of this discussion, we assume that oxygen supply is the limiting resource needed to force cells to adopt *in vivo* BMR phenotypes. We further assume that unlike the intact adipose spheroid model discussed previously, designed organs-on-a-chip utilize a space-filling microfluidic structure which provides rapid diffusional access to all portions of the tissue under study. These space-filling transportation networks typically take the form of bifurcating channels, which may be a useful tool in practically realizing this constraint. If designers of individual micro-organs are able to realize these conditions of a quantitatively limited but well-distributed supply network, we can then assume that allometric scaling principles can be applied to these metabolically realistic organs.

System overview

An overview of the proposed human-on-a-chip is outlined in Fig. 5A. In keeping with existing designs,[12,26] we suggest establishing a circulating flow of a blood substitute, which will likely be some form of cell culture media. Although a cell culture formulation capable of supporting the variety of cell types necessary in a human-on-a-chip has yet to be developed, we assume that this may be done through the use of tethered growth factors and cues. The circulating fluid can be re-oxygenated either in a specifically designed chamber or within the lung compartment, depending on the functional capabilities of the lung-on-a-chip. Oxygenated fluid can then be split into various flows to each organ based on relative cardiac output (Fig. 5B). To simplify the design of the system, we assume that the device is fabricated in some non-oxygen permeable material, such as polystyrene.[69,70] Additional mechanisms for elimination and replenishment of waste products and nutrients will also be required, if the relevant organs are unable to provide this function.

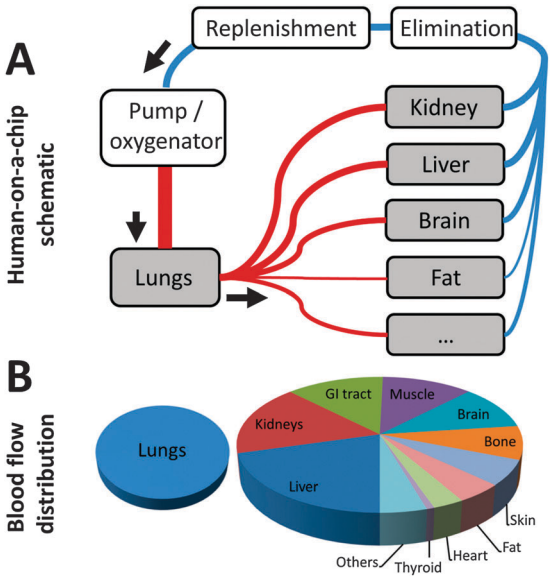

Fig. 5 (A) Schematic of a simplified human-on-a-chip flow distribution. Blood substitute is pumped through an oxygenator and a lung-on-a-chip, before being distributed to multiple organs comprising the system. The pooled liquid is collected and cycled through the system. (B) Distribution of blood flow through the organ compartments. 100% of the volume is passed through the lungs, and then split into different volumetric flow rates, reflecting blood flow distribution in a human at rest (calculated from ref. 78).

Designing the circulatory system

Blood volume scales linearly with body mass, and we use this as a starting point to design the system. The blood volume, cardiac output and cellular BMR for a miniaturized human for three selected scale factors are listed in Table 2. Since blood volume and cardiac output will dictate the pump specifications, we select a miniaturization factor of 10^4 as a plausible model system for subsequent calculations. The rapid circulation of media translates into a flow rate of 100 μL s^{-1}, and maintaining these parameters allows us to infer allometrically that the cellular BMR will be increased by an order of magnitude (given the assumptions listed above; Table 2). This issue can be circumvented by designing the blood substitute in the system to carry less oxygen than mammalian blood. Fortunately, the solubility of oxygen in cell culture media is 33-fold (or one order of magnitude) less than in blood. Hence, if the only source of oxygen in the system is the blood substitute, cells should function at a similar BMR to cells in humans. The incorporation of synthetic oxygen carriers in the blood substitute[71] may be used to fine-tune this system. In fact, designing a blood substitute to carry more oxygen would enable designers to reduce the rapid circulation flow rate to more manageable values.

Table 3 Design of 3D organs on a $10^4\times$ miniaturized human-on-a-chip using functional scaling based on maintaining metabolic rates of cells in human organs

F-3D organ	Flow rate[a] (μL s^{-1})	*In vivo* organ mass[b] (%)	$10^{-4}\times$ scaled vol (mm^3, assuming ρ = 1 g cm^{-3})	Designed[b] (mm)		
				L	*W*	*H*
Adipose	4.6	17	1250	30	21	2
Brain	8.6	2	140	25	5.6	1
Heart	3.3	0.3	33	20	1.7	1
Muscle	24.0	41	3000	30	20	5
Bone	7.1	14	1050	20	10.5	5
Thyroid	0.84	0.0003	2	2	1	1

[a] Calculated using cardiac distribution data available from Williams and Leggett (1999).[78] [b] Calculated using organ mass data for a 73 kg male.[78]

Designing organ compartments

As discussed by Wikswo and colleagues,[26] utilizing allometric scaling to design the organ compartments can yield some far-fetched results. They then suggest choosing "the size that provides the appropriate relative organ functional activity".[26] To simplify this approach, we have elected to approximate a scaling factor based on the expected functional modality of the organ. We utilize the following calculations to simply illustrate our arguments regarding scaling of multiple organ systems, based on fabrication constraints typically found in microengineered systems. The specific geometry of individual compartments depends on a variety of factors pertaining to that specific organ, and in this section we simplify these features to length, width and height.

Our approach is based on classifying organs as being either "functionally three-dimensional" (F-3D) or "functionally two-dimensional" (F-2D). This division is not based on the structure of the tissue, but on the primary function of the organ. Secretory, storage, or other functions that should scale on a per cell basis are classified as F-3D. Examples include mesenchymal tissues such as glands, the lymph nodes, bone marrow and fat. These tissue functions scale linearly with mass, and so a $10^4\times$ miniaturization prompts a reduction in organ volume by a factor of 10^4 (Table 3).

Organs that serve primarily filtration, adsorption, and gas or molecular transport functions, which are mainly mediated by epithelial cells and vascular endothelial cells, are classified as F-2D. These organs scale their function with surface area, such as in the kidneys, lungs or blood–brain barrier. Recent allometric scaling work[72] indicates that the surface area of

Table 2 Allometric scaling of circulation system components using the form $Y = Y_oM^{\alpha}$

Scale factor	Body mass α = 1	Blood volume α = 1	Cardiac output α = 3/4	Cellular BMR α = −1/4	Whole body circulation time (s)
10^0 = 1×	100 kg	5 L	100 mL s^{-1}	$10^{-11.5}$	~50
10^{-2} = 1/100×	1 kg	50 mL	3.16 mL s^{-1}	10^{-11}	~15
10^{-4} = 1/10 000×	10 g	0.5 mL	100 μL s^{-1}	$10^{-10.5}$	~5
10^{-6} = 1/1 000 000	100 mg	5 μL	3.16 μL s^{-1}	10^{-10}	~2

Table 4 Design of 2D organs on a first-generation human-on-a-chip using functional scaling based on $\alpha = 1$ allometric scaling rate for area

F-2D organ	Flow rate[a] ($\mu L\ s^{-1}$)	*In vivo* surface area (m^2)	$10^{-4}\times$ scaled area (mm^2) $\alpha = 1$	Designed (mm)			Wall shear[c] (dynes cm^{-2})	Organ volume (μL)
				L	W	H[b]		
Lung	100	70 [65]	7000	20	350	0.035	14 [9]	245
Liver	20.6	400 [79]	40 000	200	200	0.025	9.9 [80]	1000
Blood–brain barrier	8.7	20 [81]	2000	40	50	0.04	6.2 [82]	80
Kidney	21.4	0.6 [83]	60	15	4	0.15	14.2 [84]	9
Skin	5.8	2 [65]	200	20	9	0.25	4.8	45
GI tract (small intestine)	20.5	200 [85]	20 000	200	100	2.5	0.002 [86]	50 000

[a] Calculated using cardiac distribution data available from Williams and Leggett (1999).[78] [b] Heights for F-2D organ compartments assigned to control shear at the surface of the channel within physiological values (see footnote *c*). [c] Surface shear calculated using eqn (2), and designed to match values provided in the associated references within 8%. When references were unavailable, shear rates of <5 dynes cm^{-2} were used to demonstrate this scaling approach.

space-filling branched structures scales linearly ($\alpha = 1$) with the mass of the organism. This scaling factor results in far smaller organs than the 2/3 scaling factor employed when scaling the surface area of conventional geometric shapes. Hence, the only distinction between our handling of F-2D and F-3D organs is that in the F-3D case the volume is constrained, while in the F-2D case, the surface area is constrained. The height of the F-2D compartments is based on shear force requirements, using a formula relating fluid flow and channel dimensions with shear stress:

$$\tau = \frac{6\mu Q}{wh^2} \quad (2)$$

where τ is the wall shear stress, μ is the viscosity of the fluid, Q is the flow rate, w is the width of the channel and h is the height of the channel. A first approximation of these design parameters is included in Tables 3 and 4. When integrating the proposed scaling approach with PBPK-based analysis of the system, F-3D systems are consistent with 'flow-limited' compartments in which the drug or metabolite is assumed to be uniformly distributed throughout the compartment. F-2D systems represent 'membrane-limited' compartments in which mass transport and diffusion limitations play a key role.

Inherent challenges in this approach

Based on channel dimensions selected in Table 3, F-2D scaled organs require blood volume compartments substantially larger than the total blood volume of the organism. A parametric sweep of channel dimensions for the lung (Table 5) demonstrates that though we may reduce the total volume of the organ, we create greater challenges in physical implementation. For example, reducing the lung blood volume to 1/10th of the systemic blood volume requires a 1 mm long channel, which is 7 m in width and 7.5 μm in height. This width is larger than the width of any silicon wafer, and the channel height is not much greater than that of a cell, making cell culture challenging. Furthermore, these dimensions will require an immensely powerful pump, the ability to fabricate microfluidics able to withstand high pressure loads, and a bifurcating network of channels to force fluid uniformly through the lung compartment.

Significant simplifications are made in classifying the complex function of organs. Classifying organs as being either F-2D or F-3D can be problematic in cases such as the liver, which serve both secretory and adsorption functions. Furthermore, toxic side-effects may depend on the volume of an organ that has been scaled based on area. For example, the formation of a cancerous lung tumor likely depends on the volumetrically scaled number of fibroblasts present. Differences between these scaling approaches may generate a false-positive for cancerous side effects in the lung. However, this approach does provide a useful first-order approximation to scaling in these systems.

Finally, in order to implement PBPK models of this complexity, it is important to understand that all organ systems of the body must be included in the model, either explicitly or implicitly. While explicit inclusion of all organ systems is the goal of a completely generalizable human-on-a-chip, it will likely not be practically possible to capture every tissue. Hence, even in a complete "human-on-a-chip" model, additional compartments that implicitly represent 'other tissues' must be included. These additional compartments may be rapidly or slowly perfused depending on the nature of the supportive, connective or functional tissue that is missing from the explicitly defined model.

5. Potential synergies between intra- and inter-organ engineering

As demonstrated in the theoretical calculations, scaling is difficult to apply directly in designing a human-on-a-chip.

Table 5 Possible lung design configurations for a 10^{-4} scaled human-on-a-chip, compatible with maintaining F-2D scaled area and physiological shear rates

Lung design constraints	Length	Width	Height (μm)	Compartment volume (μL)	% of system blood volume
Area = 7000 mm^2, Shear = 15 dynes cm^{-2}	1 m	7 mm	240	1680	336
	10 cm	70 mm	75	525	105
	1 cm	70 cm	25	175	35
	1 mm	7 m	7.5	52.5	10.5
	100 μm	70 m	2.5	17.5	3.5

Fortunately, several engineering techniques may be applicable to circumvent these challenges, by engineering the individual organ compartments to better match the scaling requirements that exist between multiple organs.

The favorable effects of using low-oxygen carrying cell culture media instead of blood have already been discussed. By developing new blood substitutes that further decrease the amount of oxygen available per unit of blood substitute, greater volumes of blood may be used to fill the high-volume human-on-a-chip, while maintaining the same cellular BMR. While this increased volume would result in decreased concentrations of circulating components, the blood substitute may be designed to partially prevent solubility of different chemicals. A possible approach is to utilize two-phase flows, in which an inert, phase-separated fluid such as low-viscosity fluorocarbon oil can be used to supplement the blood substitute, providing greater volume without increasing the carrying capacity of solutes or dissolved gases. Similarly, the viscosity of the blood substitute can be adjusted to increase or decrease the applied shear stress on the tissues, depending on what is necessary to rationally scale the system. Such an approach would require careful consideration of the hydrophobic/hydrophilic and partitioning nature of any chemical cues present in the system.

Non-physiological 'organ assisting' systems that can augment organ function *in vitro* may also be used to rationally design a human-on-a-chip. Controlled amounts of oxygen can be supplied to cells using a network of PDMS channels[73] that are independent of the circulatory system, giving designers more freedom to adjust the circulating blood volume and organ compartment sizes. F-3D organs that secrete chemicals, such as the pancreas, can be augmented by monitoring systemic glucose levels and empirically adjusting insulin levels in the system. F-2D organs focused on filtration can be augmented using in-line dialysis or substrate-based capture methods to selectively remove components that are supposed to be cleared from the system. While these simplifications may not capture the range of functions of a real organ, they may still serve as a suitable method to obtain first-order functionality and reduce the size of some of the larger organs on the chip.

Finally, as demonstrated in the adipose spheroid experiments presented here, design of the tissue itself can have a significant impact on the scaling properties of the system. While transport-limited systems produced functional outputs that were independent of organ size, systems which allowed rapid diffusional transport followed expected scaling patterns. Individual organs in a human-on-a-chip may be designed to exploit this effect of tissue structure on scaling. For example, the miniaturization factor for a human-on-a-chip may be selected to be greater than 10^4 (as calculated in the previous section), such that the largest organ is reduced in size to physically realistic dimensions. The smaller organs will then likely be too small to construct, but this can be avoided by designing larger, diffusion-limited systems such as spheroids, in which only a small section of cells play a role in interacting with the external system, while the remaining cells provide support structures for the tissue. In this specific example, excessive adipose tissue may be included in the system, but while in compacted spheroid form, will uptake glucose in response to insulin doses at levels comparable to a less dense tissue, thereby avoiding hypoglycemic conditions.

While it is unlikely that a single 'magic bullet' will solve the scaling issues discussed here, a combination of these and other engineering innovations seems likely to beat the challenges presented in rationally designing an appropriately scaled human-on-a-chip. It seems probable that this will require individual organs to be re-engineered from the bottom-up while taking into account inter-organ relationships.

6. Conclusions

Integrating individual organs-on-a-chip into a single 'human-on-a-chip' for drug efficacy and toxicological screening applications is a challenging venture, and designing the scale of interacting organs to mimic human physiology is a critical step in realizing this technology. Our simple experiments in the fat–insulin–glucose metabolism system demonstrate that appropriate scaling is necessary to maintain physiological levels of glucose within the blood, and that the design of tissue structure within the organ-on-a-chip is intrinsically linked with the scaling approaches necessary to connect multiple organs in a realistic fashion. Specifically, tissue structure controls transport of materials into and out of cells, and designing transport-limited organs can negate the effects of scaling in the system. Hence, in engineering multiple organs, design specifications at both the intra- and inter-organ levels need to be considered. We theoretically explore inter-organ scaling, and while existing approaches may be used to test very specific hypotheses, we explore the possibility of designing a 'generalized' human-on-a-chip. In particular, we suggest that focusing on basal metabolic rates, which is the physiological cellular end result of allometric scaling of organ sizes, be given just as high a priority as designing organs to be correctly scaled relative to each other. Given the importance of metabolic rate in controlling cell function, this 'metabolically supported functional scaling' approach may be more applicable to a variety of scenarios. This novel and simple scaling model serves as a first order approximation for the complex calculations necessary to precisely and accurately recapitulate human physiology. We demonstrate that practical application of these scaling approaches is challenging, but engineering workarounds can be developed to circumvent these issues, by designing individual organs from the bottom-up to contribute towards a rationally designed human-on-a-chip.

7. Experimental methods

Spheroid culture

Mouse pre-adipocyte cell line (3T3-L1) was obtained from ATCC (ATCC# CL-173) and maintained in growth medium consisting of Dulbecco's Modified Eagle's Medium (DMEM, Gibco, cat#11965) supplemented with 10% newborn calf serum (Gibco, cat#26010066) and 1% penicillin/streptomycin/glutamine (Gibco, cat#10378-016). Low passage cell stocks (P4 to P8) were used for all

experiments to ensure robust adipogenic response. Adipose spheroids were fabricated using a custom molded 384-hanging drop plate, as previously described.[74] Briefly, 3T3-L1 cells were rinsed with Hank's balanced salt solution (Gibco, cat#14175103) and trypsinized (Gibco, cat#25200056) to yield a single cell suspension. After centrifugation, cells were resuspended in growth medium containing 0.32% w/v MethoCel™ A4M (Dow Corning, Midland, MI), and then seeded in a 384-well hanging drop plate, giving initial cell seeding concentrations of 6.4×10^4 (64k) cells per spheroid. The addition of MethoCel™ prevents cells from adhering to the hanging drop plate and enhances spheroid formation. At 2 days post-seeding, the growth medium was replaced with adipose differentiation medium consisting of DMEM supplemented with 10% fetal bovine serum (Gibco #16000044), 10 nM triiodothyronine, 10 μM troglitazone, 0.25 μM dexamethasone and 1 μg mL^{-1} insulin (all from Sigma) and cultured for 3 days, after which the medium was replaced with DMEM supplemented with 10% FBS and 1 μg mL^{-1} insulin, and changed once every 2 days until day 9 post-seeding. Finally, the spheroids were starved overnight at day 9 post-seeding in serum-free, Hank's Balanced Saline Solution (HBSS, Gibco cat#14025) and used for experiments on day 10 post-seeding.

Viability analysis

Viability of cells contained in 64k spheroids was assessed by pooling ~20 spheroids in a tube. Spheroids were treated with a solution of 1 mg mL^{-1} collagenase I (Worthington Biochemical) and mechanically dispersed into a solution of PBS containing 4 μM calcein AM and 2 μM ethidium homodimer. Cells were incubated in the Live/Dead reagents for 30 minutes at room temperature, and spotted on a glass microscope slide. The percentage of live (dead) cells was assessed by counting the number of cells stained green (red) using a fluorescent microscope.

Chip fabrication

The microfluidic chips used for all experiments consisted of 0.1 mm tall by 1 mm wide inlet channels connected to an open 3 mm-diameter chamber (Fig. 2). Microfluidic channels were fabricated using conventional soft lithography.[75] Briefly, a mold was produced using SU-8 (Microchem) photolithography on silicon wafers, using protocols described by the manufacturers. The poly(dimethylsiloxane) (PDMS) base and the curing agent (Sylgard 184, Dow Corning) were mixed in a 10 : 1 ratio by weight, degassed, and poured over the SU-8 mold. After curing at 60 °C overnight, the PDMS channels were cut, and a 3 mm biopsy punch was used to core out the chamber. The PDMS device was then bonded to glass slides using a plasma cleaner (Covance MP-1, Femto Science), and placed in a 120 °C oven to increase bonding strength and decrease hydrophilicity of the treated device.

Chip operation

To run an insulin–glucose assay, device chambers were filled with collagen gels containing either intact or dispersed differentiated spheroids. 64k spheroids were dispersed by incubating in a solution of 1 mg mL^{-1} collagenase 4 (Worthington Biochemical) in HBSS at 37 °C for 5–10 minutes and disrupted mechanically by repeated pipetting. Three dispersed or intact spheroids (1.92×10^5 cells per chamber) were re-suspended in 20 μL collagen gel precursor solution (500 μL type I bovine collagen (BD Biosciences), 60 μL 10× phosphate buffered saline, 50 μL 0.8 M $NaHCO_3$; stored on ice until ready for use), loaded into the central chamber with a pipette, and allowed to gel for 15 minutes at 37 °C. In addition, a series of samples containing 1/10 the number of dispersed cells per flow chamber (1.92×10^4 cells per chamber) were also constructed to investigate the effect of cell density on insulin stimulated glucose uptake. An array of 100 μm diameter posts similar to those described by Jeon and colleagues[76] was designed to keep the cell-laden collagen precursor from flowing into either the inlet or outlet channels. After loading, the flow chamber was kept open to allow the perfusate to pool over the collagen gel. The chip was perfused with normal glucose (5.5 mM) HBSS containing 10 μg mL^{-1} insulin at a constant flow rate of 1 μL min^{-1}. After 25 minutes of flow, 5 μL of perfusate was collected and stored on ice for later analysis. To minimize air bubbles and synchronize the start times of each chip, the device was primed by bringing the insulin-supplemented HBSS to the edge of the chamber prior to loading the chamber with the collagen–cell mixture.

Glucose assay

Consumption of glucose by differentiated adipose tissues was determined by Amplex™ red glucose assay (Invitrogen, cat#A22189). Perfusate from the microfluidic chip was collected and diluted 200-fold in phosphate buffered saline (PBS; Gibco). The diluted samples were then loaded into 96-well microtiter plates and mixed with the reaction mixture according to the protocols from the manufacturer. Samples for a standard curve (50 μM to 0 μM glucose) were generated by diluting HBSS of a known glucose concentration (5.5 mM) with PBS. Once the reaction was complete, sample fluorescence was determined using a BioTek Neo plate reader at 530EX/590EM, and converted to glucose concentrations using the standard curve. Values are reported as means ± standard error, for n = 7–8 samples.

Statistical analysis

Data were analyzed for outliers using Pierce's method as described by Ross.[77] Briefly, the test statistic consisted of the ratio between the difference of a single data point from the mean and the standard deviation of the data set. If the test statistic for any given data point exceeded a predetermined threshold that point was deemed an outlier and removed from the analysis. A 2-tailed t-test with $\alpha = 0.05$ was used to determine significance.

Acknowledgements

We would like to thank Professor Michael Shuler for helpful comments and Andrew Hartman for assistance with cell culture. The authors gratefully acknowledge personal support from the Natural Sciences and Engineering Research Council of

Canada and the Banting postdoctoral fellowship programs to CM, and the University of Michigan Microfluidics in Biomedical Sciences Training Program (NIH T32 EB005582-05) to JML. This project was supported by the NIH ((GM096040, CA170198 (ST)); and R01-DK095137 (THC)) and by the Defense Threat Reduction Agency (DTRA) and Space and Naval Warfare Command Pacific (SSC PACIFIC) under Contract No. N66001-13-C-2027. Any opinions, findings and conclusions or recommendations expressed in this material are those of the author(s) and do not necessarily reflect the views of the DTRA and SSC PACIFIC.

References

1 D. Huh, Y. Torisawa, G. A. Hamilton, H. J. Kim and D. E. Ingber, *Lab Chip*, 2012, **12**, 2156.
2 C. Moraes, G. Mehta, S. C. Lesher-Perez and S. Takayama, *Ann. Biomed. Eng.*, 2012, **40**, 1211–1227.
3 J. H. Sung, M. B. Esch, J.-M. Prot, C. J. Long, A. Smith, J. J. Hickman and M. L. Shuler, *Lab Chip*, 2013, **13**, 1201–1212.
4 C. Moraes, Y. Sun and C. A. Simmons, *Integr. Biol.*, 2011, **3**, 959–971.
5 N. J. Douville, P. Zamankhan, Y.-C. Tung, R. Li, B. L. Vaughan, C.-F. Tai, J. White, P. J. Christensen, J. B. Grotberg and S. Takayama, *Lab Chip*, 2011, **11**, 609–619.
6 J. W. Song, S. P. Cavnar, A. C. Walker, K. E. Luker, M. Gupta, Y.-C. Tung, G. D. Luker and S. Takayama, *PLoS One*, 2009, **4**, e5756.
7 M. Nikkhah, F. Edalat, S. Manoucheri and A. Khademhosseini, *Biomaterials*, 2012, **33**, 5230–5246.
8 A. L. Hook, D. G. Anderson, R. Langer, P. Williams, M. C. Davies and M. R. Alexander, *Biomaterials*, 2010, **31**, 187–198.
9 D. Huh, B. D. Matthews, A. Mammoto, M. Montoya-Zavala, H. Y. Hsin and D. E. Ingber, *Science*, 2010, **328**, 1662–1668.
10 D. Huh, H. Fujioka, Y. C. Tung, N. Futai, R. Paine, J. B. Grotberg and S. Takayama, *Proc. Natl. Acad. Sci. U. S. A.*, 2007, **104**, 18886–18891.
11 J. H. Sung and M. L. Shuler, *Ann. Biomed. Eng.*, 2012, **40**, 1289–1300.
12 M. B. Esch, T. L. King and M. L. Shuler, *Annu. Rev. Biomed. Eng.*, 2011, **13**, 55–72.
13 I. Roberts, I. Kwan, P. Evans and S. Haig, *Br. Med. J.*, 2002, **324**, 474–476.
14 J. Seok, H. S. Warren, A. G. Cuenca, M. N. Mindrinos, H. V. Baker, W. Xu, D. R. Richards, G. P. McDonald-Smith, H. Gao, L. Hennessy, C. C. Finnerty, C. M. López, S. Honari, E. E. Moore, J. P. Minei, J. Cuschieri, P. E. Bankey, J. L. Johnson, J. Sperry, A. B. Nathens, T. R. Billiar, M. A. West, M. G. Jeschke, M. B. Klein, R. L. Gamelli, N. S. Gibran, B. H. Brownstein, C. Miller-Graziano, S. E. Calvano, P. H. Mason, J. P. Cobb, L. G. Rahme, S. F. Lowry, R. V. Maier, L. L. Moldawer, D. N. Herndon, R. W. Davis, W. Xiao, R. G. Tompkins, A. Abouhamze, U. G. J. Balis, D. G. Camp, A. K. De, B. G. Harbrecht, D. L. Hayden, A. Kaushal, G. E. O'Keefe, K. T. Kotz, W. Qian, D. A. Schoenfeld, M. B. Shapiro, G. M. Silver, R. D. Smith, J. D. Storey, R. Tibshirani, M. Toner, J. Wilhelmy, B. Wispelwey and W. H. Wong, *Proc. Natl. Acad. Sci. U. S. A.*, 2013, **110**, 3507–3512.
15 W. Yin, E. Carballo-Jane, D. G. McLaren, V. H. Mendoza, K. Gagen, N. S. Geoghagen, L. A. McNamara, J. N. Gorski, G. J. Eiermann, A. Petrov, M. Wolff, X. Tong, L. C. Wilsie, T. E. Akiyama, J. Chen, A. Thankappan, J. Xue, X. Ping, G. Andrews, L. A. Wickham, C. L. Gai, T. Trinh, A. A. Kulick, M. J. Donnelly, G. O. Voronin, R. Rosa, A.-M. Cumiskey, K. Bekkari, L. J. Mitnaul, O. Puig, F. Chen, R. Raubertas, P. H. Wong, B. C. Hansen, K. S. Koblan, T. P. Roddy, B. K. Hubbard and A. M. Strack, *J. Lipid Res.*, 2012, **53**, 51–65.
16 A. P. Li, C. Bode and Y. Sakai, *Chem.-Biol. Interact.*, 2004, **150**, 129–136.
17 A. P. Li, *ALTEX*, 2008, **25**, 33–42.
18 K. Viravaidya, A. Sin and M. L. Shuler, *Biotechnol. Prog.*, 2004, **20**, 316–323.
19 C. Zhang, Z. Zhao, N. A. A. Rahim, D. van Noort and H. Yu, *Lab Chip*, 2009, **9**, 3185.
20 Y. Imura, E. Yoshimura and K. Sato, *Anal. Sci.*, 2012, **28**, 197–199.
21 P. M. van Midwoud, M. T. Merema, E. Verpoorte and G. M. M. Groothuis, *Lab Chip*, 2010, **10**, 2778.
22 D. Mazzei, M. a. Guzzardi, S. Giusti and A. Ahluwalia, *Biotechnol. Bioeng.*, 2010, **106**, 127–137.
23 B. Vinci, D. Cavallone, G. Vozzi, D. Mazzei, C. Domenici, M. Brunetto and A. Ahluwalia, *Biotechnol. J.*, 2010, **5**, 232–241.
24 J. B. S. Haldane, *Possible worlds*, Chatto and Windus, London, 1927.
25 J. H. Sung and M. L. Shuler, *Lab Chip*, 2009, **9**, 1385–1394.
26 J. Wikswo, F. E. Block, D. E. Cliffel, J. Enders, C. R. Goodwin, C. C. Marasco, D. A. Markov, D. L. McLean, J. A. McLean, J. McKenzie, R. S. Reiserer, P. C. Samson, D. Schaffer, K. T. Seale and S. Sherrod, *IEEE Trans. Biomed. Eng.*, 2013, **60**, 682–690.
27 O. Snell, *Arch. Psychiatr. Nervenkrankh.*, 1892, **23**, 436–446.
28 D. W. Thompson, *On Growth and Form*, Cambridge University Press, Dover, 1917.
29 P. B. Reich, M. G. Tjoelker, J.-L. Machado and J. Oleksyn, *Nature*, 2006, **439**, 457–461.
30 M. Kleiber, *Physiol. Rev.*, 1947, **27**, 511–541.
31 S. F. Noujaim, *Circulation*, 2004, **110**, 2802–2808.
32 G. B. West, *Science*, 1997, **276**, 122–126.
33 G. B. West, *Science*, 1999, **284**, 1677–1679.
34 G. B. West, *J. Exp. Biol.*, 2005, **208**, 1575–1592.
35 G. B. West, *Proc. Natl. Acad. Sci. U. S. A.*, 2002, **99**, 2473–2478.
36 V. M. Savage, J. Gillooly, W. Woodruff, G. West, A. Allen, B. Enquist and J. Brown, *Funct. Ecol.*, 2004, **18**, 257–282.
37 V. M. Savage, E. J. Deeds and W. Fontana, *PLoS Comput. Biol.*, 2008, **4**, e1000171.
38 T. Sbrana and A. Ahluwalia, *New Technologies for Toxicity Testing*, 2012, pp. 138–153.

39 F. Vozzi, J. M. Heinrich, A. Bader and A. D. Ahluwalia, *Tissue Eng., Part A*, 2008, **15**, 1291–1299.
40 M. A. Guzzardi, F. Vozzi and A. D. Ahluwalia, *Tissue Eng., Part A*, 2009, **15**, 3635–3644.
41 M. A. Guzzardi, C. Domenici and A. Ahluwalia, *Tissue Eng., Part A*, 2011, **17**, 1635–1642.
42 E. Iori, B. Vinci, E. Murphy, M. C. Marescotti, A. Avogaro and A. Ahluwalia, *PLoS One*, 2012, **7**, e34704.
43 F. Hyder, D. L. Rothman and M. R. Bennett, *Proc. Natl. Acad. Sci. U. S. A.*, 2013, **110**, 3549–3554.
44 R. S. Balaban, *Proc. Natl. Acad. Sci. U. S. A.*, 2013, **110**, 3216–3217.
45 S. Herculano-Houzel, *PLoS One*, 2011, **6**, e17514.
46 J. R. Banavar, A. Maritan and A. Rinaldo, *Nature*, 1999, **399**, 130–132.
47 V. M. Savage, A. P. Allen, J. H. Brown, J. F. Gillooly, A. B. Herman, W. H. Woodruff and G. B. West, *Proc. Natl. Acad. Sci. U. S. A.*, 2007, **104**, 4718–4723.
48 J. R. Banavar, M. E. Moses, J. H. Brown, J. Damuth, A. Rinaldo, R. M. Sibly and A. Maritan, *Proc. Natl. Acad. Sci. U. S. A.*, 2010, **107**, 15816–15820.
49 O. Toussaint, G. Weemaels, F. Debacq-Chainiaux, K. Scharffetter-Kochanek and M. Wlaschek, *J. Cell. Physiol.*, 2011, **226**, 315–321.
50 L. M. Sweeney, M. L. Shuler, J. G. Babish and A. Ghanem, *Toxicol. In Vitro*, 1995, **9**, 307–316.
51 J. H. Sung, C. Kam and M. L. Shuler, *Lab Chip*, 2010, **10**, 446–455.
52 A. Sin, K. C. Chin, M. F. Jamil, Y. Kostov, G. Rao and M. L. Shuler, *Biotechnol. Prog.*, 2004, **20**, 338–345.
53 P. Trayhurn and J. H. Beattie, *Proc. Nutr. Soc.*, 2001, **60**, 329–339.
54 V. Poitout, J. Amyot, M. Semache, B. Zarrouki, D. Hagman and G. Fontés, *Biochim. Biophys. Acta*, 2010, **1801**, 289–298.
55 M. A. Scott, V. T. Nguyen, B. Levi and A. W. James, *Stem Cells Dev.*, 2011, **20**, 1793–1804.
56 G. J. Todaro and H. Green, *J. Cell Biol.*, 1963, **17**, 299–313.
57 M. Inoue, L. Chang, J. Hwang, S.-H. Chiang and A. R. Saltiel, *Nature*, 2003, **422**, 629–633.
58 C. S. Rubin, A. Hirsch, C. Fung and O. M. Rosen, *J. Biol. Chem.*, 1978, **253**, 7570–7578.
59 J. R. Wu-Wong, C. E. Berg, J. Wang, W. J. Chiou and B. Fissel, *J. Biol. Chem.*, 1999, **274**, 8103–8110.
60 A. R. Saltiel and C. R. Kahn, *Nature*, 2001, **414**, 799–806.
61 T.-H. Chun, K. B. Hotary, F. Sabeh, A. R. Saltiel, E. D. Allen and S. J. Weiss, *Cell*, 2006, **125**, 577–591.
62 R.-Z. Lin and H.-Y. Chang, *Biotechnol. J.*, 2008, **3**, 1172–1184.
63 A. C. Daquinag, G. R. Souza and M. G. Kolonin, *Tissue Eng., Part C*, 2012, **19**, 336–344.
64 D. Vishwanath, H. Srinivasan, M. S. Patil, S. Seetarama, S. K. Agrawal, M. N. Dixit and K. Dhar, *J. Cell Commun. Signaling*, 2013, **7**, 129–140.
65 J. E. Hall and A. C. Guyton, *Textbook of medical physiology*, Saunders, Philadelphia, Pa. London, 2010.
66 M. X. Zuber, S. M. Wang, K. V. Thammavaram, D. K. Reed and B. C. Reed, *J. Biol. Chem.*, 1985, **260**, 14045–14052.
67 J. M. Olefsky, *J. Clin. Invest.*, 1976, **57**, 842–851.
68 V. Sharma and J. H. McNeill, *Br. J. Pharmacol.*, 2009, **157**, 907–921.
69 E. W. K. Young, E. Berthier, D. J. Guckenberger, E. Sackmann, C. Lamers, I. Meyvantsson, A. Huttenlocher and D. J. Beebe, *Anal. Chem.*, 2011, **83**, 1408–1417.
70 E. Berthier, E. W. K. Young and D. Beebe, *Lab Chip*, 2012, **12**, 1224–1237.
71 J. Simoni, *Artif. Organs*, 2012, **36**, 123–126.
72 A. Wirkes, K. Jung, M. Ochs and C. Muhlfeld, *J. Appl. Physiol.*, 2010, **109**, 1662–1669.
73 J. F. Lo, E. Sinkala and D. T. Eddington, *Lab Chip*, 2010, **10**, 3291–3295.
74 Y.-C. Tung, A. Y. Hsiao, S. G. Allen, Y. Torisawa, M. Ho and S. Takayama, *Analyst*, 2011, **136**, 473.
75 D. C. Duffy, J. C. McDonald, O. J. A. Schueller and G. M. Whitesides, *Anal. Chem.*, 1998, **70**, 4974–4984.
76 C. P. Huang, J. Lu, H. Seon, A. P. Lee, L. A. Flanagan, H.-Y. Kim, A. J. Putnam and N. L. Jeon, *Lab Chip*, 2009, **9**, 1740–1748.
77 S. M. Ross, *J. Eng. Technol.*, 2003, 38–41.
78 L. R. Williams and R. W. Leggett, *Clin. Phys. Physiol. Meas.*, 1989, **10**, 187–217.
79 E. Kuntz and H.-D. Kuntz, *Hepatology: Principles and Practice; History, Morphology, Biochemistry, Diagnostics, Clinic, Therapy*, Springer Verlag, 2006.
80 T. Torii, M. Miyazawa and I. Koyama, *Transplant. Proc.*, 2005, **37**, 4575–4578.
81 D. R. Peterson, *eLS*, John Wiley & Sons, Ltd, 2001.
82 L. Cucullo, M. Hossain, V. Puvenna, N. Marchi and D. Janigro, *BMC Neurosci.*, 2011, **12**, 40.
83 A. Bohle, B. Aeikens, A. Eenboom, L. Fronholt, W. R. Plate, J.-C. Xiao, A. Greschniok and M. Wehrmann, *Kidney Int.*, 1998, **67**, S186–S188.
84 B. J. Ballermann, A. Dardik, E. Eng and A. Liu, *Kidney Int.*, 1998, **67**, S100–S108.
85 J. M. DeSesso and C. F. Jacobson, *Food Chem. Toxicol.*, 2001, **39**, 209–228.
86 H. J. Kim, D. Huh, G. Hamilton and D. E. Ingber, *Lab Chip*, 2012, **12**, 2165–2174.